Origin of femtosecond laser induced periodic nanostructure on diamond

A. Abdelmalek, B. Sotillo, Z. Bedrane, V. Bharadwaj, S. Pietralunga, R. Ramponi, E.-H. Amara, and S. M. Eaton

Citation: AIP Advances **7**, 105105 (2017); doi: 10.1063/1.5001942

View online: https://doi.org/10.1063/1.5001942

View Table of Contents: http://aip.scitation.org/toc/adv/7/10

Published by the American Institute of Physics

Origin of femtosecond laser induced periodic nanostructure on diamond

A. Abdelmalek,[1,a] B. Sotillo,[2] Z. Bedrane,[1] V. Bharadwaj,[2] S. Pietralunga,[2] R. Ramponi,[2] E.-H. Amara,[3] and S. M. Eaton[2]
[1]*Physics Department, Theoretical Physics Laboratory, Tlemcen University, 13000 Tlemcen, Algeria*
[2]*IFN-CNR and Dipartimento di Fisica, Politecnico di Milano, 20133 Milano, Italy*
[3]*Laser Material Processing Team, Centre for Advanced Technologies Development, CDTA, PO. Box 17, Baba-Hassen 16303, Algiers, Algeria*

(Received 11 May 2017; accepted 1 October 2017; published online 9 October 2017)

We study the evolution of periodic nanostructures formed on the surface of diamond by femtosecond laser irradiation delivering 230 fs pulses at 1030 nm and 515 nm wavelengths with a repetition rate of 250 kHz. Using scanning electron microscopy, we observe a change in the periodicity of the nanostructures by varying the number of pulses overlapping in the laser focal volume. We simulate the evolution of the period of the high spatial frequency laser induced periodic surface structures at the two wavelengths as a function of number of pulses, accounting for the change in the optical properties of diamond via a generalized plasmonic model. We propose a hypothesis that describes the origin of the nanostructures and the principal role of plasmonic excitation in their formation during multipulse femtosecond laser irradiation. https://doi.org/10.1063/1.5001942

I. INTRODUCTION

Laser–induced periodic surface structures (LIPSS) have attracted considerable attention by researchers, as indicated by the growth in the number of papers published on the topic in recent years.[1] LIPSS can enhance the absorption[2–5] at the surface of materials and can therefore open new avenues for technological applications such as micro–solar cells devices. LIPSS formation is a universal phenomenon and has been observed in dielectrics, semiconductors, metals and polymers.[1,6] Generally, two types of ripples can be observed during the irradiation by multipulse femtosecond laser, low spatial frequency LIPSS (LSFL) and high spatial frequency LIPSS (HSFL).

Derrien *et al.*[10] used an above ablation threshold fluence where the critical density of plasmonic excitation is achieved with the first femtosecond laser pulse. They observed ablation in the middle of the laser spot surrounded by LSFL and at the edge where the fluence is low, they found the HSFL. So we suggest that this repartition of the two kinds of LIPSS observed within the same volume spot laser are the result of different physical mechanisms.

LSFL formation for the majority of materials is well explained by the interference between the incident laser wave and the surface plasmon-polariton (SPP) excitation,[1,7,8] which involves a periodic spatial modulation of the energy deposited on the irradiated surface.[9,10] This interaction leads to the formation of nanostructures with periods close to or less than the laser wavelength λ_L. There is still some controversy in the literature regarding the physical mechanisms underlying the formation of HSFL. The physical models proposed include interference,[10,11] second harmonic generation (SHG)[12,13] and surface plasmon polariton excitation.[14–18]

[a]Electronic mail: ahmed7abdelmalek13@gmail.com

TABLE I. Data from literature for the observed LIPSS periods in different materials.

Wavelength (nm)	target	Dielectric environment	HSFL period (nm)	Ref.
800	Si	Water	400–150	15
800	I-b diamond	Air	200–50	19
800	DLC[a]	Air	170–60	14

[a]Diamond–Like Carbon.

The interference model depends necessarily on the angle of the incident laser, but it has been shown that the incident angle has no effect in the case of HSFL formation.[8,12] The SHG model is based on the formula: $\Lambda = \frac{\lambda_L}{2n}$ and so the nanostructure period depends strictly on the wavelength. In contrast, there are several experimental works where a change in the period of the HSFL has been observed by varying the pulse number at the same wavelength (Tab. I).

Miyazaki *et al.*[15] and Miyaji *et al.*[14,16,17] proposed a model for HSFL formation where they consider the effect of the number of pulses. They proved experimentally that the formation of nanostructures was due to a non-thermal process, where the random nanoablation is initiated by the disorder (non-thermal melting) during the multipulse femtosecond laser irradiation, followed by plasmonic excitation. In this model, a large number of laser pulses at low energy are necessary to generate HSFL type.[13,15] Forster *et al.*[19] showed a 50 nm period obtained due to a phase transition from crystalline diamond to a graphitic phase, along with 200 nm nanostructures consisting of crystalline diamond (see Tab. I). Clearly, a more sophisticated model is needed to provide insight into the formation of HSFL.

In this paper, we investigate the change in diamond surface morphology induced by ultrafast laser pulses when varying the scanning speed (i.e. number of pulses per spot size diameter) and the laser power (fluence) at 1030 nm and 515 nm wavelength. We illustrate the advantage of using plasmonic excitation in modeling the HSFL formation. We propose a general plasmonic model to follow the evolution of LIPSS formation and the changing diamond optical properties as a function of the electron-holes plasma excitation. Our model demonstrates the importance of plasmonic excitation in the dynamic change of non-thermal melting as an origin of HSFL formation.

II. EXPERIMENTAL SETUP

The samples used in this work were polished single crystal CVD diamond 7.5 mm × 7.5 mm × 0.5 mm. Their optical properties are discussed later in the theoretical model. To irradiate the diamond we used a Light Conversion Pharos amplified femtosecond laser delivering 230 fs pulses at 1030 nm and 515 nm wavelengths with a repetition rate of 250 kHz. The laser was incident normal to the target surface and focused with a 0.42 NA (50×) microscope objective, with a spot size of approximately 1.6 μm and 0.8 μm at 1030 nm and 515 nm wavelengths, respectively. To investigate the creation of surface nanostructures we varied the pulse number by changing the scanning speed, v, through the relationship: $N = \frac{2\omega_0 R_r}{v}$ where R_r is the repetition rate, $2\omega_0$ is the spot size and N the number of pulses delivered per spot diameter.[20] The laser polarization was parallel to the scanning direction, and all the experiments were carried out in air. After the irradiation, we analyzed the change in morphology of diamond surfaces using a scanning electron microscope (SEM).

III. THEORETICAL MODEL

We propose a generalized plasmonic model to study the development of periodical nanostructures on diamond surface during the irradiation with multipulse femtosecond laser at wavelengths of 1030 nm and 515 nm. We consider air as the dielectric environment. The plasmonic model has shown its validity in the case of metals.[35] Applying this model to semiconductors and dielectrics such as diamond is justified by the fact that a thin layer which has metallic character is induced during multipulse femtosecond laser irradiation.[27] In this paper, we call it "pseudo-metal layer". For this reason, the surface plasmon polariton SPP excitation is used to calculate and explain the formation

of periodic nanostructures in diamond. The SPP dispersion relation is:[21]

$$\omega^2 = c^2 k_{sp}^2 \frac{(\varepsilon_{pm} + \varepsilon_d)}{\varepsilon_{pm}\varepsilon_d}. \tag{1}$$

where ε_{pm} is the dielectric function of pseudo-metal layer and $k_{sp} = k_{sp1} + ik_{sp2}$ is the plasmon propagation number with $k_{sp1} = \Re k_{sp} = \frac{2\pi}{\lambda_{sp}} = \frac{\pi}{\Lambda}$ (Ref. 18) where λ_{sp} is the plasmon wavelength and Λ is the period of nanostructures and ε_d is the dielectric function of the material surrounding the pseudo-metal layer. This dielectric function is approximated as $\varepsilon_d = m\varepsilon_{di} + (1 - m)\varepsilon_{air}$ where m represents the factor of mixed state depending implicitly on the pulse number and it varies from 0 and 1, $\varepsilon_{air} = 1$ and $\varepsilon_{di} = 5.72$ and 5.90 at 1030 nm and 515 nm wavelengths, respectively, according to the relationship $n^2 = 1 + \frac{0.3306\lambda^2}{\lambda^2 - 175^2} + \frac{4.3356\lambda^2}{\lambda^2 - 106^2}$ (λ in nm) with $\varepsilon_{di} = n^2$ (Ref. 22). The dielectric function of the pseudo-metal layer is given by the Drude model:[23]

$$\varepsilon_{pm} = \varepsilon_{pm1} + i\varepsilon_{pm2} = 1 + (\varepsilon_{di} - 1)(1 - \frac{n_{eh}}{n_0}) - \frac{\omega_p^2}{\omega^2}\frac{1}{1 + \frac{i}{\omega\tau_{ee}}}. \tag{2}$$

with

$$\varepsilon_{pm1} = 1 + (\varepsilon_{di} - 1)(1 - \frac{n_{eh}}{n_0}) - \frac{\omega_p^2}{\omega^2}\frac{1}{1 + \frac{1}{\omega^2\tau_{ee}}}. \tag{3}$$

$$\varepsilon_{pm2} = \frac{1}{\omega\tau_{ee}}\frac{\omega_p^2}{\omega^2}\frac{1}{1 + \frac{1}{\omega^2\tau_{ee}}}. \tag{4}$$

where n_0 is the electron concentration in the valence band (we consider a value of 10^{23} cm^{-3}), τ_{ee} the electron-electron collision time (1 fs), ω is laser frequency and $\omega_p = \sqrt{\frac{n_{eh}e^2}{\varepsilon_0 m_{opt}^* m_e}}$ is plasma frequency, with $\varepsilon_0 = 8.85 \times 10^{-12}$ F.m and the optical effective mass m_{opt}^* estimated via the relationship[23] $m_{opt}^* = (m_e^{*-1} + m_h^{*-1})^{-1} = 0.30$ with $m_e^* = 3(m_{le}^{-1} + m_{te}^{-1} + m_{te}^{-1})^{-1}$ and $m_h^* = \frac{(m_{hh}^{\frac{3}{2}} + m_{lh}^{\frac{3}{2}})}{(m_{hh}^{\frac{1}{2}} + m_{lh}^{\frac{1}{2}})}$ (Ref. 24) being m_{le}, m_{te}, m_{hh}, m_{lh} being equal to 1.4, 0.36, 1.1, 0.3 (Refs. 25 and 26), respectively, for our single crystal CVD diamond.

M. Straub *et al.*[18] determined the groove period of Si after constructing the numerical formulas for k_{sp1} and k_{sp2} using the critical density of plasmon excitation n_{cr} for the purpose to simplify the calculations, such as $k_{sp1}(n_{cr}) = 0$. In our case is $n_{cr} = 2.32 \times 10^{21}$ cm^{-3} and 7.58×10^{21} cm^{-3} at λ_L = 1030 nm, 515 nm, respectively, but their formulas become valid only for the properties of Si and the wavelength used. In this paper, without employing the critical density n_{cr}, we will build the general formulas of k_{sp1} and k_{sp2} adapted for all semiconductor and dielectric materials and for all wavelengths.

According to Eq. (1)

$$k_{sp}^2 = \frac{\omega^2}{c^2}\frac{\varepsilon_{pm}\varepsilon_d}{\varepsilon_{pm} + \varepsilon_d}. \tag{5}$$

And

$$k_{sp}^2 = (k_{sp1} + ik_{sp2})^2 = k_{sp1}^2 - k_{sp2}^2 + i2k_{sp1}k_{sp2}. \tag{6}$$

$$\frac{1}{k_{sp1}^2} = \frac{c^2}{\omega^2}(\frac{1}{\varepsilon_d} + \frac{1}{\varepsilon_{pm}}). \tag{7}$$

$$\frac{1}{k_{sp1}^2} = \frac{c^2}{\omega^2}(\frac{\varepsilon_{pm1}^2 + \varepsilon_{pm2}^2 + \varepsilon_d\varepsilon_{pm1} - i\varepsilon_d\varepsilon_{pm2}}{\varepsilon_d(\varepsilon_{pm1}^2 + \varepsilon_{pm2}^2)}). \tag{8}$$

$$k_{sp1}^2 = \frac{\omega^2}{c^2}(\frac{\varepsilon_d(\varepsilon_{pm1}^2 + \varepsilon_{pm2}^2)}{\varepsilon_{pm1}^2 + \varepsilon_{pm2}^2 + \varepsilon_d\varepsilon_{pm1} - i\varepsilon_d\varepsilon_{pm2}}). \tag{9}$$

We set:

$$\alpha = \varepsilon_{pm1}^2 + \varepsilon_{pm2}^2 + \varepsilon_d \varepsilon_{pm1}, \quad \beta = \varepsilon_d \varepsilon_{pm2} \text{ and } \gamma = \varepsilon_d (\varepsilon_{pm1}^2 + \varepsilon_{pm2}^2)$$

Which implies:

$$k_{sp1}^2 = \frac{\omega^2}{c^2}\left(\frac{\gamma}{\alpha - i\beta}\right) = \frac{\omega^2}{c^2}\left(\frac{\gamma(\alpha + i\beta)}{\alpha^2 + \beta^2}\right). \tag{10}$$

We also have:

$$k_{sp1}^2 - k_{sp2}^2 = \frac{\omega^2}{c^2}\frac{\gamma\alpha}{\alpha^2 + \beta^2}. \tag{11}$$

$$2k_{sp1}k_{sp2} = \frac{\omega^2}{c^2}\frac{\gamma\beta}{\alpha^2 + \beta^2}. \tag{12}$$

$$(12) \longrightarrow k_{sp2}^2 = \left(\frac{\omega^2}{2c^2 k_{sp1}}\right)^2 \frac{\gamma^2\beta^2}{(\alpha^2 + \beta^2)^2}. \tag{13}$$

Replacing Eq. (13) in Eq. (11), we obtain:

$$4k_{sp1}^4 - 4\frac{\omega^2}{c^2}\frac{\gamma\alpha}{(\alpha^2 + \beta^2)}k_{sp1}^2 - \left(\frac{\omega^2}{c^2}\right)^2 \frac{\gamma^2\beta^2}{(\alpha^2 + \beta^2)^2} = 0. \tag{14}$$

The solution of Eq. (14) is:

$$k_{sp1} = \frac{1}{\sqrt{2}}\frac{\omega}{c}\left[\frac{\gamma\alpha}{(\alpha^2 + \beta^2)} + \frac{\gamma}{(\alpha^2 + \beta^2)^{\frac{1}{2}}}\right]^{\frac{1}{2}}. \tag{15}$$

Therefore, from Eq. (12) we obtain:

$$k_{sp2} = \frac{\omega^2}{2c^2 k_{sp1}}\frac{\gamma\beta}{(\alpha^2 + \beta^2)}. \tag{16}$$

This model was simulated using MATLAB software.

IV. RESULTS AND DISCUSSION

Diamond surface excitation by femtosecond laser pulses builds up a thin pseudo-metal layer[27] due to the non-thermal melting (disorder) which takes place at sub-vibrational time scale, since the pulse duration of the femtosecond laser is lower than the electron-phonon relaxation time.[27–31] This change of states affects optical properties of diamond such as reflectivity R, as shown in Fig. 1, with $R = \frac{(n-1)^2+k^2}{(n+1)^2+k^2}$, where $n = \frac{1}{\sqrt{2}}\left[\varepsilon_{pm1} + (\varepsilon_{pm1}^2 + \varepsilon_{pm2}^2)^{\frac{1}{2}}\right]^{\frac{1}{2}}$ is the real part of the refractive index and $k = \frac{\varepsilon_{pm2}}{2n}$ is the absorption coefficient.[32] We observe an increase of the reflectivity as a function

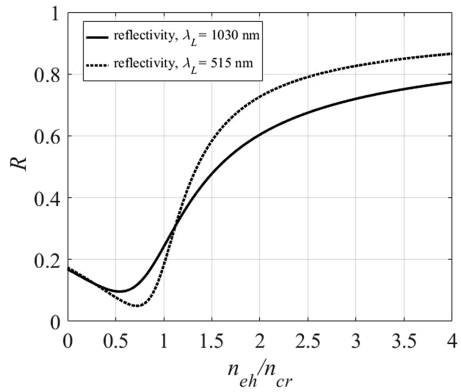

FIG. 1. The reflectivity of the pseudo-metal layer in diamond as a function of the electron-hole plasma density at both wavelengths.

of the excited electron-hole plasma density n_{eh} during the multipulse femtosecond laser interaction, where the reflectivity R is calculated for normal incident radiation. This indicates that the diamond surface takes a metallic character with high free electron density. We can remark that the reflectivity at 515 nm is higher than 1030 nm due to the difference in electron density excited (note that x-axis is different for each plot because $n_{cr}(1030\ \text{nm}) \neq n_{cr}(515\ \text{nm})$).

Under our experimental conditions, we have observed morphological changes of the femtosecond laser irradiated diamond surface with the variation of the scanning speed v (i.e. number of pulses N) at a fixed fluence F, always keeping the laser polarization parallel to the translation direction of the sample. Figure 2 shows SEM images taken on the irradiated diamond surface for the two selected wavelengths. According to these images, the femtosecond laser is inducing nanostructures with sub-wavelength period (HSFL) perpendicular to the polarization of the laser beam. Previous results suggest that random nanoablation would result from the lattice disorder and intense near-field.[14,16] However, we have observed in experiment an ordered nanostructure and therefore we suggest that a periodic process is responsible for the ordering of the nanoablation. Moreover, we observed in Fig. 2 that the period of the nanostructure decreases when the number of pulse increases. With each incident femtosecond laser pulse, the density of excited electrons increases, resulting in a decrease of the real part of dielectric function of the irradiated layer, allowing for plasmonic excitation. Therefore, we suggest that the formation of HSFL can be attributed initially to the excitation of SPP in the surface layer. From our simulations, we show the importance of the plasmonic excitation on the formation of the HSFL, and also shed insight into other physical processes involved. It can also be observed in Fig. 2 that there is ablation of the material at the center of the micro-grooves, where the peak fluence of the Gaussian beam is highest. This effect is more noticeable for lower scan speeds, as heat accumulation is more pronounced for a greater number of pulses interacting within the focal volume in the pseudo-metal layer.[20] Despite the ablation at the center of the tracks, nanostructures can be observed at the sides of the micro-grooves, indicating that the periodic nanostructures are produced at fluences slightly below the ablation threshold.[11]

Figure 3 shows SEM images of the HSFL formed with fluences ranging from 7.96, 8.36 and 9.15 J/cm^2 (average laser power 20, 21 and 23 mW) at 1030 nm wavelength. The periods of the nanostructures decreases slightly with increasing fluence, owing to a strong disorder of the lattice

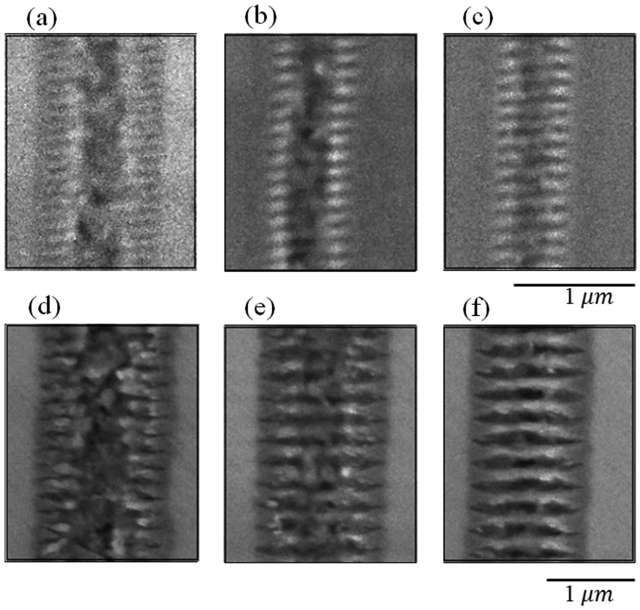

FIG. 2. SEM images of diamond surfaces irradiated with femtosecond laser pulses polarized parallel to the scan direction for (a) v = 3 mm/s, (b) v = 6.5 mm/s, (c) v = 8 mm/s at λ_L= 515 nm and fluence (power) F= 6.36 J/cm^2 (4 mW), (d) v = 3 mm/s, (e) v = 6 mm/s, and (f) v = 8 mm/s at λ_L= 1030 nm and fluence (power) F= 8.36 J/cm^2 (21 mW).

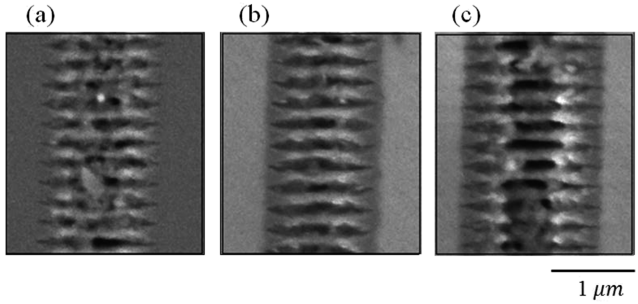

FIG. 3. SEM images of diamond surfaces irradiated with the parallel polarized laser pulses at λ_L=1030 nm with v = 8 mm/s at (a) F= 7.96 J/cm^2, (b) F= 8.36 J/cm^2 and (c) F= 9.15 J/cm^2 (power 20, 21 and 23 mW respectively).

during the interaction with the femtosecond laser, which is attributed to the incubation of nano-ripples when greater energy density is delivered to the lattice.

Figure 4 shows a recapitulation of the effect of fluence (power) and speed (number of pulses) on the nanostructure period for 515 nm (a) and 1030 nm (b) wavelengths. The period of the nanostructures increases with scan speed for both wavelengths. The minimum period is 110 nm and 190 nm for 515 nm and 1030 nm wavelengths, respectively, for the lowest speed (3 mm/s). From this, we deduce that the formation of nano-ripples has a strong dependence on the wavelength, with the period increasing with wavelength.

One can also observe, according to Fig. 4, that the nanostructures are not obtained for all values of fluence or speeds, due to the large band gap of diamond (5.5 eV), where the electrons can be excited by one photon if it has enough energy, or by a multiphoton absorption if the photon energy is below the gap.[33] To observe nanostructures for powers lower than 4 mW (F = 6.36 J/cm^2) at 515 nm writing wavelength Fig. 4(a), we need to increase the number of pulses by decreasing the scan speed. However at the green wavelength, we found a narrower energy window between ablation and no modification, making it more difficult to observe the formation of nanostructures.

Next we simulate the evolution of the periodicity of nanostructure HSFL type via the generalized plasmonic model proposed above. When the pulse number increases, the excited electron density n_{eh} increases until the condition $\varepsilon_{pm} = -\varepsilon_{air}(m = 0)$ is reached. At this point, the **F**irst **O**rdered **N**anostructure (**FON**) can be observed, with a period of Λ_{FON} = 250 nm at λ_L = 515 nm (Fig. 5(a)), and a period of Λ_{FON} = 510 nm at λ_L = 1030 nm (Fig. 5(b)). This corresponds to the minimum Plasmon Resonance RP_{min}. This RP_{min} is caused when the plasmons tend to coherently couple with the incident laser wave at the pseudo–metal/air interface as if the original material (diamond) did not exist.

The smallest nanostructure or the **L**ast **O**rdered **N**anostructure (**LON**) can be observed when $\varepsilon_{pm} = -\varepsilon_{di}(m = 1)$ with period of Λ_{LON} = 83 nm and 197 nm at wavelength 515 and 1030 nm, respectively (Fig. 5). This corresponds to the maximum Plasmon Resonance RP_{max}. In the data shown in Fig. 5, we are varying the factor of mixed state for 0 to 1 for the purpose of seeing the

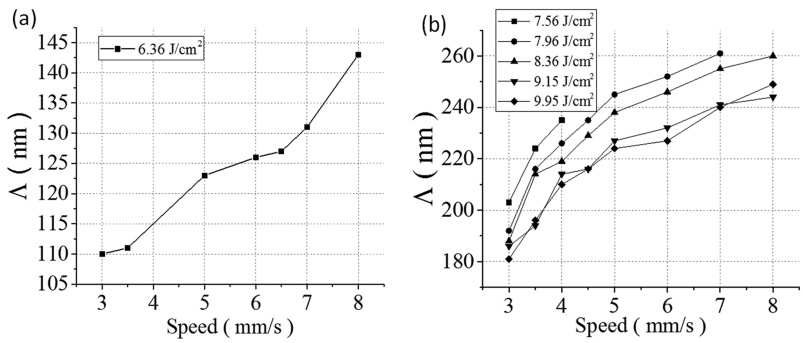

FIG. 4. Evolution of periodicity with writing speed and fluence at wavelength 515 nm (a) and 1030 nm (b).

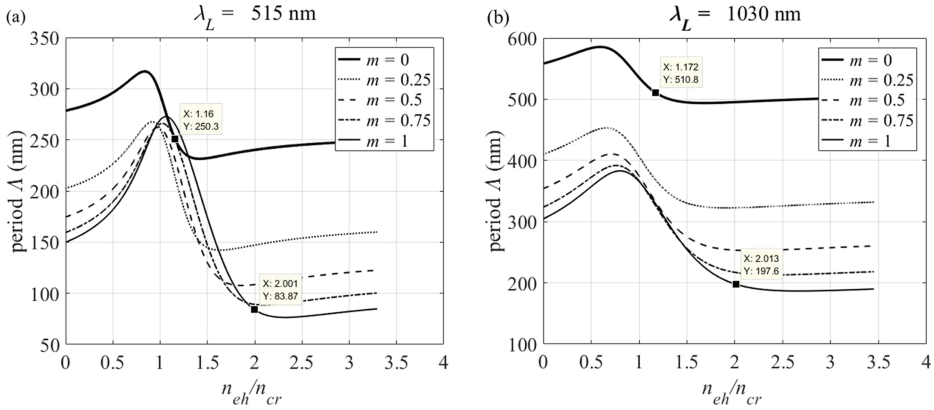

FIG. 5. Calculation of LIPSS period evolution as a function of electron-hole plasma excitation by varying the dielectric surrounding medium, at wavelength 515 nm (a) and 1030 nm (b). X is the fraction n_{eh}/n_{cr} correspond to $\varepsilon_{pm} = -\varepsilon_{air}$ or $-\varepsilon_{di}$ where Y is the period, then (X, Y) represent **FON** or **LON**.

effect of the penetration of plasmonic evanescent wave at both interfaces of the pseudo-metal layer on the periodicity of the nanostructures with the increase of the number of incident laser pulses. Fig. 6 shows the penetration depth of the irradiated wave as a function of electron-hole plasma excitation, $d = \frac{c}{2\omega k}$ (Ref. 18) where all the parameters were previously defined. d is the penetration depth of laser during the irradiation. When the number of pulses increases, the density of excited electrons and the absorption coefficient k increase, then the penetration depth decreases. Based on (Fig. 6), the depth of the pseudo-metal layer is tens of nanometers. Therefore, the pseudo metal layer remains a mix state (from the point of view of the dielectric function) between air and bulk diamond when ε_{pm} decrease from $-\varepsilon_{air}$ to $-\varepsilon_{di}$. Therefore, we can assume that there is a transverse migration of the SPP from the pseudo-metal/air interface to the diamond/pseudo-metal as the number of femtosecond laser pulses increases, where the nanostructure period decreases from Λ_{FON} to Λ_{LON}. So we deduce that the ordered nanostructures (HSFL type) can be observed only inside the range $[RP_{\min}, RP_{\max}]$. It is important to note that this model is valid in a specific carrier density corresponding to the plasmonic excitation. Our experimental results are in agreement with these calculations, where the measured periods (Fig. 4) are included in the plasmonic range calculated for the both wavelengths (Fig. 5). The period Λ_{LON} is also called saturation period as it is the minimum pitch of the nanostructures.[34]

We have highlighted in Fig. 6 the case corresponding to $RP_{\min}$ and $RP_{\max}$. So based on our reasoning above the d_{max} which corresponds to $RP_{\max}$ is the smallest depth possible, taking on values $d_{max} = 61$ nm, 32 nm at $\lambda_L = 1030$ nm, 515 nm respectively, therefore, all the absorbed energy at the pseudo-metal layer with depth d_{max} to be reserved to the SPP excitation, and this is why the period Λ_{LON} can enhance the surface absorption.[4,5] Thus, it is important to find this period if the aim is to

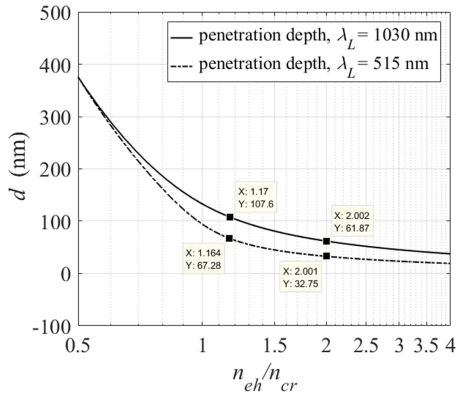

FIG. 6. Penetration depth of the irradiated wave as a function of electron-hole plasma excitation at both wavelengths.

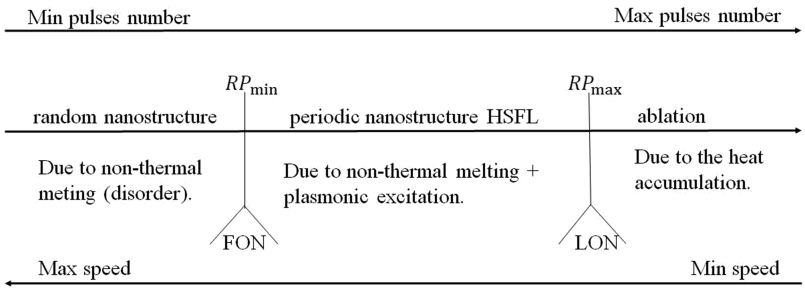

FIG. 7. Evolution of nanostructure formation with the increase in the number of pulses (i.e. reduction of speed).

obtain high efficiency micro–solar cells with femtosecond laser pulses, to avoid energy dissipation inside the material. It has been confirmed experimentally that with only LIPSS the absorption can be enhanced to more than 90% via plasmonic excitation,[2–5] because the plasmons wave oscillateds at a scale of λ_{sp} which is less than λ_L. Therefore, the plasmons are able to efficiently absorb the incident light, i.e. they are able to respond together at the same point of time and space to the incident radiation.

Our model for the formation of HSFL in diamond during the interaction with femtosecond laser pulses can also be applied in general to dielectrics and semiconductors, taking into account the effect of plasmonic excitation in non-thermal melting dynamics. Experimental results show that the period of the nanostructures decreases when the number of laser pulses increases. On the other hand, during the analysis of the LIPSS period versus the electron-hole plasma excitation, we see that the period Λ decreases when the factor of mixed states m decreases until reaching the saturation at the maximum Plasmonic Resonance RP_{max}. This implies that the pseudo–metal layer transitions from crystalline diamond to a graphitic phase occurs progressively when the period decreases from Λ_{FON} to Λ_{LON}. As this transition is due to non-thermal melting (disorder),[19] we can conclude that the ordered nanostructures are formed by a combination of two processes: the random nanoablation due to the near field induced during irradiation, and the plasmonic excitation, that plays a complementary and simultaneous role to order the nanoablation because of its specific wave periodicity (frequency).

Finally, as the random nanostructures are generated by random disorder, it can be called ordinary disorder, while as HSFL are due to disorder forced by the plasmon wave, it can be called plasmonic disorder. The overview of this description is presented in Fig. 7, which also helps to summarize the physical processes involved in the formation of the HSFL during the irradiation with femtosecond laser pulses. It is shown that the origin of random nanostructures is related to one process (disorder), in contrast to order nanostructures of HSFL type that are related to a combination of two processes (disorder + plasmonic excitation).

V. CONCLUSION

In this paper, we have studied the origin of the formation of periodic nanostructures (HSFL) by femtosecond laser pulses on the surface of diamond. The experimental results have shown that the periodicity observed depends on the pulse number for both wavelengths used (1030 nm and 515 nm). We suggest that the non-thermal melting (disorder) and plasmonic excitation have a very important role in the dynamic process. We propose a generalized plasmonic model that can be used directly to simulate the evolution of periodic nanostructure HSFL for dielectric or semiconductor materials at any wavelength. Using this model for the particular case of diamond allows us to calculate the period of nanostructures formed on the surface, and we have confirmed with the experimental results that the period decreases when the number of pulses increases via the variation of both carrier density and the mixed state factor. We conclude that the periodic nanostructures can only be observed in the range of plasmonic excitation bounded by a minimum and maximum plasmon resonance [RP_{min}, RP_{max}], whereas random nanostructures can be formed below RP_{min}. Finally, we propose a physical description that shows the importance of plasmonic excitation in the formation of

sub-wavelength nanostructures, where the plasmonic excitation effect for non-thermal melting dynamics (disorder) can be considered as a fundamental process for the periodic nanoablation as origin of HSFL nanostructures.

[1] J. Bonse, S. Höhm, S. V. Kirner, A. Rosenfeld, and J. Krüger, "Laser-induced periodic surface structures—A scientific evergreen," IEEE J. Sel. Topics Quantum Electron **23**, 9000615 (2017).
[2] A. Y. Vorobyev and C. Guo, "Enhanced absorptance of gold following multipulse femtosecond laser ablation," Phys. Rev. B **72**, 195422 (2005).
[3] A. Y. Vorobyev and C. Guo, Solar absorber surfaces treated by femtosecond laser, *Biosciences (BIOSCIENCESWORLD), IEEE International Conference*, 135 (2010).
[4] P. Calvani, A. Bellucci, M. Girolami, S. Orlando, V. Valentini, A. Lettino, and D. M. Trucchi, "Optical properties of femtosecond laser-treated diamond," App. Phys. A **117**, 25 (2014).
[5] P. Calvani, A. Bellucci, M. Girolami, S. Orlando, V. Valentini, R. Polini, and D. M. Trucchi, "Black diamond for solar energy conversion," Carbon **105**, 401 (2016).
[6] E. Rebollar, J. R. V. de Aldana, I. Martín-Fabiani, M. Hernández, D. R. Rueda, T. A. Ezquerra, C. Domingo, P. Moreno, and M. Castillejo, "Assessment of femtosecond laser induced periodic surface structures on polymer films," Physical Chemistry Chemical Physics **15**, 11287 (2013).
[7] M. Huang, F. Zhao, Y. Cheng, N. Xu, and Z. Xu, "Origin of laser-induced near-subwavelength ripples: Interference between surface plasmons and incident laser," ACS Nano **3**, 4062 (2009).
[8] Q. Wu, Y. Ma, R. Fang, Y. Liao, Q. Yu, X. Chen, and K. Wang, "Femtosecond laser-induced periodic surface structure on diamond film," Phys. Rev. Lett **82**, 1703 (2003).
[9] T. Chen, H. Yang, E. Zhao, J. Qian, J. Hao, J. Han, W. Tang, and H. Zhu, "Laser induced nanostructures on the zinc surface," Journal of Russian Laser Research **35**, 561 (2014).
[10] T. J.-Y. Derrien, R. Koter, J. Krüger, S. Höhm, A. Rosenfeld, and J. Bonse, Plasmonic formation mechanism of periodic 100-nm-structures upon femtosecond laser irradiation of silicon in water, J. Appl. Phys **116**, 074902 (2014).
[11] M. Shinoda, R. R. Gattass, and E. Mazur, "Femtosecond laser-induced formation of nanometer width grooves on synthetic single-crystal diamond surfaces," Appl. Phys **105**, 053102 (2009).
[12] D. Dufft, A. Rosenfeld, S. K. Das, R. Grunwald, and J. Bonse, "Femtosecond laser-induced periodic surface structures revisited: A comparative study on ZnO," J. Appl. Phys **105**, 034908 (2009).
[13] R. Le Harzic, F. Stracke, and H. Zimmermann, "Formation mechanism of femtosecond laser-induced high spatial frequency ripples on semiconductors at low fluence and high repetition rate," J. Appl. Phys **113**, 183503 (2013).
[14] G. Miyaji and K. Miyazaki, "Origin of periodicity in nanostructuring on thin film surfaces ablated with femtosecond laser pulses," Opt. Express **16**, 16265 (2008).
[15] K. Miyazaki and G. Miyaji, "Periodic nanostructure formation on silicon irradiated with multiple low-fluence femtosecond laser pulses in water," Physics Procedia **39**, 674 (2012).
[16] G. Miyaji and K. Miyazaki, "Role of multiple shots of femtosecond laser pulses in periodic surface nanoablation," Appl. Phys. Lett **103**, 071910 (2013).
[17] G. Miyaji and K. Miyazaki, "Fabrication of 50-nm period gratings on GaN in air through plasmonic near-field ablation induced by ultraviolet femtosecond laser pulses," Opt. Express **24**, 4648 (2016).
[18] M. Straub, M. Afshar, D. Feili, H. Seidel, and K. König, "Surface plasmon polariton model of high-spatial frequency laser-induced periodic surface structure generation in silicon," J. Appl. Phys. **111**, 124315 (2012).
[19] M. Forster, C. Huber, O. Armbruster, R. Kalish, and W. Kautek, "50-nanometer femtosecond pulse laser induced periodic surface structures on nitrogen-doped diamond," Diamond and Related Materials **74**, 114 (2017).
[20] S. M. Eaton, H. Zhang, M. Li Ng, J. Li, W.-J. Chen, S. Ho, and P. R. Herman, "Transition from thermal diffusion to heat accumulation in high repetition rate femtosecond laser writing of buried optical waveguides," Opt. Express **16**, 9443 (2008).
[21] *Near-field optics and surface plasmon polaritions*, edited by S. Kawata (Springer, Berlin, 2001), p. 19.
[22] *Optical Properties of Diamond*, edited by A. M. Zaitsev (Springer, Bochum, 2001).
[23] K. Sokolowski-Tinten and D. von der Linde, "Generation of dense electron-hole plasmas in silicon," Phys. Rev. B **61**, 2643 (2000).
[24] *Diamond: Electronic Properties And Applications*, edited by L. S. Pan and D. R. Kania (New York, 1995), pp. 251–252.
[25] F. Nava, C. Canali, C. Jacoboni, L. Reggiani, and S. F. Kozlov, "Electron effective masses and lattice scattering in natural diamond," Solid State Communications **33**, 475 (1980).
[26] L. Reggiani, S. Bosi, C. Canali, F. Nava, and S. F. Kozlov, "On the lattice scattering and effective mass of holes in natural diamond," Solid State Communications **30**, 333 (1979).
[27] G. Miyaji, W. Kobayashi, and K. Miyazaki, "Reflectivity change in nanoscale modification of DLC film with femtosecond laser pulses," J. Laser Micro Nanoeng **2**, 146 (2007).
[28] G. Sciaini, M. Harb, S. G. Kruglik, T. Payer, C. T. Hebeisen, F.-J. M. z. Heringdorf, M. Yamaguchi, M. H.-v. Hoegen, R. Ernstorfer, and R. J. D. Miller, "Electronic acceleration of atomic motions and disordering in bismuth," Nature **458**, 56 (2009).
[29] S. K. Sundaram and E. Mazur, "Inducing and probing non-thermal transitions in semiconductors using femtosecond laser pulses," Nature Materials **1**, 217 (2002).
[30] C. V. Shank, R. Yen, and C. Hirlimann, "Time-resolved reflectivity measurements of femtosecond-optical- pulse induced phase transitions in silicon," Phys. Rev. Lett **50** (1983).
[31] T. Zier, E. S. Zijlstra, A. Kalitsov, I. Theodonis, and M. E. Garcia, "Signatures of nonthermal melting," Structural Dynamics **2**, 054101 (2015).
[32] *Handbook of Optical Constants of Solids*, edited by E. D. Palik (Elsevier, Academic Press, USA, 1985), p. 192.

[33] D. Von der Linde, K. Sokolowski-Tinten, and J. Bialkowski, "Laser–solid interaction in the femtosecond time regime," Applied Surface Science **109**, 1 (1997).
[34] S. Richter, M. Heinrich, S. Döring, A. Tnnermann, and S. Nolte, "Formation of femtosecond laser-induced nanogratings at high repetition rates," Appl. Phys. A **104**, 503 (2011).
[35] F. Garrelie, J. P. Colombier, F. Pigeon, S. Tonchev, N. Faure, M. Bounhalli, S. Reynaud, and O. Parriaux, "Evidence of surface plasmon resonance in ultrafast laser-induced ripples," Optics Express **19**, 9035 (2011).